Surface Structure Sensitivity of the Water−Gas Shift Reaction on Cu(*hkl*) Surfaces: A Theoretical Study

Guichang Wang,*,† Ling Jiang,† Zunsheng Cai,† Yinming Pan,† Xuezhuang Zhao,*,† Wei Huang,‡ Kechang Xie,‡ Yongwang Li,§ Yuhan Sun,§ and Bing Zhong§

Department of Chemistry, Nankai University, Tianjin, 300071, People's Republic of China, Taiyuan University of Technology, Taiyuan, 030024, People's Republic of China, and Institute of Coal Chemistry, Chinese Academy of Science, Taiyuan, 030001, People's Republic of China

Received: July 8, 2002; In Final Form: September 30, 2002

The surface structure sensitivity of the water−gas shift (WGS) reaction ($CO + H_2O \rightarrow CO_2 + H_2$) over the Cu(111), Cu(100), and Cu(110) surfaces has been studied by first-principles density functional calculations together with the UBI-QEP approach. The Cu(*hkl*) surfaces are simulated by the Cu_{10} and Cu_{14} cluster models. The selectivity of the WGS reaction on the well-defined single-crystal surfaces is closely associated with the differences in the dissociation energies of H_2O on the metal surfaces. The trend in the calculated dissociation energies and activation barriers follows the order Cu(110) < Cu(100) < Cu(111), suggesting that the most efficient crystal surface for catalyzing the WGS reaction is Cu(110), closely followed by the Cu(100) surface, and that the more densely packed Cu(111) surface is the least active among the Cu(*hkl*) surfaces studied here. The present calculations are in good agreement with experimental observations.

1. Introduction

The water−gas shift (WGS) reaction ($CO + H_2O \rightarrow CO_2 + H_2$) is frequently applied in the chemical process industry; it also plays a secondary role in many proposed future technologies for energy conversion (e.g., coal conversion to liquid fuels).[1] The so-called "low-temperature" Cu/ZnO catalyst is widely used to catalyze this reaction. The WGS reaction has been studied over both high-surface-area catalysts containing Cu and ZnO[2−7] and model catalysts based on Cu single crystals, which have very well controlled surface cleanliness and geometric structure.[8,9] Those studies show that metallic Cu provides the active site for catalysis.[8,9]

Generally, two different mechanisms (i.e., a formate mechanism and a "surface redox" mechanism) may be used to elucidate the WGS reaction. Some authors support the former, whereby surface hydroxyls (OH_a) produced from dissociatively adsorbed H_2O combine with adsorbed CO (CO_a) to produce a surface formate intermediate ($HCOO_a$), which then decomposes to $^1/_2H_2$ and CO_2.[2−5] Other authors[6−10] favor a surface redox mechanism, whereby H_2O dissociatively adsorbs to produce oxygen adatoms (O_a) and H_2, followed by the well-known reaction of CO with O_a to produce CO_2 (ref 9 and references therein). Very recently, the microkinetics of the WGS reaction has been investigated by Fishtik and Datta[11] by utilizing the conventional transition-state theory along with the unity bond index quadratic-exponential potential (UBI-QEP) method, indicating that the formate and associative mechanisms are dominant at lower temperatures whereas the redox mechanism is dominant at higher temperatures. Interestingly, the rate-determining step in each mechanism is the dissociative adsorption of water.

Real materials used in applications normally expose a number of different crystallographic faces. Also, the understanding of such a complicated system requires information about the reactivity of the particular orientations of surfaces that are involved. The sensitivity of surface reactions to the crystallographic orientation of the surface is an interesting subject for the understanding of catalysts. This is a major purpose in the application of surface science techniques to the well-defined surfaces. Kuijpers[12] reported that the WGS reaction over silica-supported copper catalysts was structurally sensitive. However, detailed explanations of this experimental phenomenon could not be found in the literature.

The interaction of atomic oxygen with metal surfaces is the basis for a number of important technological process such as bulk oxidation, corrosion, and heterogeneous catalysis (i.e., the WGS reaction). The location of these atoms at a crystal surface is fundamental to the description of surface processes. Atomic adsorption on the low-index faces of metal surfaces superficially causes the simplest type of surface structural problem. So far, the adsorption of atomic oxygen on Cu(111), Cu(100), and Cu(110) has been investigated with a variety of experimental techniques and theoretical methods, including LEED, STM, PhD, FP-LMTO, and DFT.[13−23] A good review can be found in ref 13. A few of the most important points will be cited with more recent results. However, no systematic work on the analysis of the binding characteristics of atomic oxygen adsorbed on the Cu(*hkl*) surfaces can be found in the literature to our knowledge.

A property of general interest is the difference in the adsorption energy of an adsorbate on different single-crystal surfaces. In our previous report,[24] the interactions of C, H, O, and S atoms with the Cu(111) surface have been systematically studied from first-principle density functional calculations, and the results agree well with the experiments. We feel that model calculations of atom−surface interactions can sometimes be as accurate as experiment, or they can at least complement each

* Corresponding authors. E-mail: wangguichang@eyou.com and zhaoxzh@nankai.edu.cn.
† Nankai University.
‡ Taiyuan University of Technology.
§ Institute of Coal Chemistry.

10.1021/jp0215567 CCC: $25.00
Published on Web 12/12/2002

other and supply more-accurate input data for the BOC[25,26] model method. Considering that the intrinsic fundamental phenomenon of the interaction of atomic oxygen with metal surfaces is closely related to the adsorption of water, we will employ density functional techniques to study the equilibrium geometry and the binding characteristics of atomic oxygen on the Cu(111), Cu(100), and Cu(110) surfaces. A theoretically comparative study of these systems would be of interest in evaluating the variation in catalytic ability corresponding to the WGS reaction. Because it is difficult to locate the transition states of the WGS reaction on these surfaces, we focus mainly on an evaluation of the surface dissociation energies of adsorbed water, which should be an important determining factor in the WGS reaction. Shustorovich[25] has developed the so-called bond-order conservation Morse potential (BOC-MP) method to treat the dissociations of adsorbates on metal surfaces. Also, the analytical BOC-MP equation relates the activation energy to the adsorption energies of an adsorate and its dissociative fragments. Recently, Shustorovich and Sellers[26] have made a considerable revision to the BOC-MP method with the new name of unity-quadratic exponential potential (UBI-QEP). However, the analytical expression for estimating activation barriers remains unchanged. The UBI-QEP approach is somewhat simple, but it is a reasonable way to estimate the energy barriers quickly.[26] We refer the reader to the work of Shustorovich and Sellers[26] for an in-depth discussion of the UBI-QEP approach.

2. Cluster Models and Computational Methods

The development of modern surface science provided the opportunity to investigate the interactions between catalysts and molecules or atoms on the atomic scale. However, computations of molecules containing transition-metal atoms have proven to be more difficult than those for first- and second-row atoms.[27] Recent advances in methodology based on the technologies of pseudopotential and plane-wave basis sets and high-speed computers have now made it possible to obtain quantitative information on surface phenomena. In this work, cluster models of the surface have been employed to simulate O atoms adsorbed on the Cu(111), Cu(100), and Cu(110) surfaces.

The $Cu_{10}(7, 3)$ (i.e., seven atoms in the first layer and three atoms in the second layer) and $Cu_{14}(9, 4, 1)$ (i.e., nine atoms in the first layer, four atoms in the second layer, and one atom in the third layer) cluster models, shown in Figure 1, have been chosen to represent the Cu(111), Cu(100), and Cu(110) surfaces, respectively. The Cu(111), Cu(100), and Cu(110) surfaces are constructed using the bulk lattice constant[28] of 3.615 Å. Generally, there are four different adsorption sites on the Cu(111) crystal surface: the atop site, which resides above a surface atom, two 3-fold hollow sites, which correspond to the fcc site and the hcp site (the hcp site resides above an atom of the second substrate layer; the fcc site does not), and the bridge site, which lies halfway between the fcc and hcp sites. Similarly, the 4-fold hollow site, short bridge (SB) or long bridge (LB) site, and the top site can be found on the Cu(100) and Cu(110) surfaces. These sites are schematically illustrated in Figure 1. In the present calculations, a single oxygen atom is placed on each of the different sites, namely, the top (1), bridge (1−2), hcp (1−2−7−8), fcc (1−2−3), SB (1−2), LB (1−4), and 4-fold (1−6−7−8) hollow sites (the numbers in parentheses are the same as the label for the metal atoms in Figure 1). Geometry optimizations for the perpendicular distance of the O atom to the first metal layer are carried out while the cluster geometries are fixed at the bulk lattice parameters because of the fact that

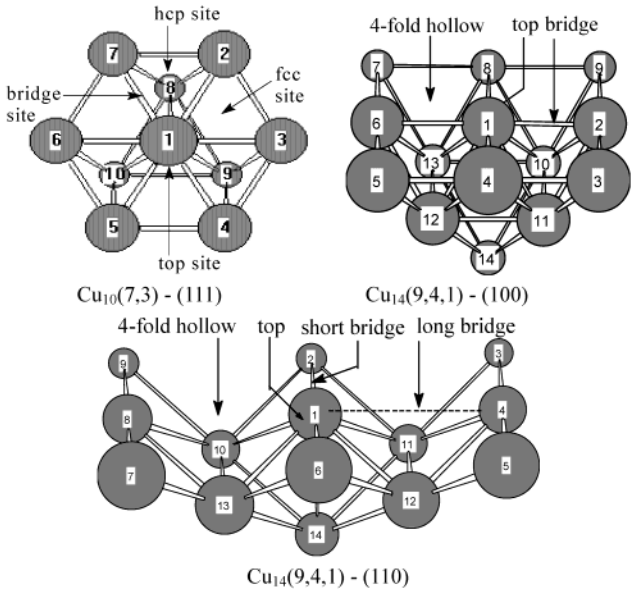

Figure 1. $Cu_{10}(7, 3)$ and $Cu_{14}(9, 4, 1)$ cluster models represent the Cu(111), Cu(100), and Cu(110) surfaces with different adsorption sites, respectively, (i.e., the top, bridge, hcp, fcc, 4-fold hollow, short bridge, and long bridge sites).

there is very little modification of the metal surface by the adatom at low coverage.[29]

The interaction of the O atom with the different adsorption sites on Cu(111), Cu(100), and Cu(110) surfaces has been studied by first-principle density functional calculations that use the hybrid B3LYP exchange-correction functional[30,31] as implemented in Gaussian 94.[32] For Cu atoms, the relativistic effective core potentials (ECP) reported by Hay and Wadt[33] have been used to describe the 1s−2p core whereas the electrons arising from the 3s, 3p, 3d, 4s, and 4p shells are treated explicitly. It is customary to refer to these ECPs as LANL2. The standard double-ζ basis set, also reported by Hay and Wadt[33] and denoted as usual by LANL2DZ, is used to describe the electron density of the valence electrons of Cu. On the basis of a close scrutiny of the basis-set effect in our previous study,[34] the electron density of the O atom is described with the standard 6-31G basis set.

The natural bond orbital (NBO) procedure[35,36] provides an efficient method for obtaining bonds and lone-pair electrons, which comprise an optimized Lewis structure of a molecule from modern ab initio wave functions. The set of orthonormal NBOs forms a compact and stable representation of the electron density in a molecule[37] and provides a convenient basis for investigating charge transfer or hyperconjugative interactions in molecular systems.[36] Reed et al.[37] report that the natural population analysis is an alternative to conventional Mulliken population analysis and seems to describe the charge distributions in compounds of high ionic character (i.e., those containing metal atoms) better, where Mulliken populations often seriously contradict the density integration and empirical measures of ionicity. In view of these cases, the NBO method[38] is employed in the analysis of the electron configuration and the binding characteristics of the O/Cu(*hkl*) adsorption systems. The adsorption energies of OH and H_2O and related activation barriers are calculated by the UBI-QEP method.

3. Results and Discussion

3.1. Preferred Site and Adsorption Energy of Atomic Oxygen. Table 1 lists the adsorption energies, natural charges,

TABLE 1: Adsorption Energies, Natural Charges, and Structural Parameters for the Adsorption of Atomic Oxygen onto the Cu(111), Cu(100), and Cu(110) Surfaces[a]

Cu(111) surface	Z_{eq}/Å	E_{ads}(DFT)/eV	Q(O)	E_{ads}(exptl)/eV
top	1.85	3.41	−1.08	
bridge	1.49	3.72	−1.20	
hcp hollow	1.36	4.30	−1.21	
fcc hollow	1.33	4.42	−1.26	4.47
Cu(100) surface	Z_{eq}/Å	E_{ads}(DFT)/eV	Q(O)	
top	1.78	4.33	−1.22	
bridge	1.41	5.33	−1.29	
4-fold hollow	0.93	5.72	−1.33	
Cu(110) surface	Z_{eq}/Å	E_{ads}(DFT)/eV	Q(O)	
top	1.76	4.68	−1.27	
short bridge	1.35	5.60	−1.30	
4-fold hollow	0.65	6.04	−1.36	
long bridge	0.51	6.55	−1.42	

[a] Z_{eq} is the perpendicular distance of the O atom to the first metal plane; E_{ads} is the adsorption energy of atomic oxygen calculated from the first-principle DFT method; Q(O) is the natural charge on atomic oxygen; and E_{ads}(exptl) is the experimental value for the adsorption energy of atomic oxygen taken from ref 52.

and structural parameters of atomic oxygen adsorbed onto each of the sites on the Cu(111), Cu(100), and Cu(110) surfaces, together with available experimental data. The adsorption energy (E_{ads}) is calculated according to the equation

$$E_{ads} = E(\text{cluster}) + E(\text{O}) - E(\text{cluster} + \text{O}) \qquad (1)$$

where E(cluster), E(O), and E(cluster + O) denote the calculated energy of a cluster without an O atom, a free O atom, and a cluster with an O atom, respectively. A positive value of E_{ads} implies that the adsorption of an O atom from the gas phase is thermodynamically favorable.

To find the preferred site for atomic oxygen, we first examine its adsorption behavior on the Cu(111) surface. The optimized results show that the oxygen atom prefers to stay outside the surface. The perpendicular distances between the oxygen atom and the first copper layer range from 1.33 to 1.85 Å. In fact, on the fcc (111) surface, the 3-fold hollow sites are so tightly packed and the metal interlayer spacing is so small that the adatoms usually do not penetrate deeply enough to form a direct bond with a metal atom in the second metal layer.[26] For the fcc hollow site, the calculated adsorption energy for an O atom (4.42 eV) agrees well with the experimental value (4.47 eV). However, the adsorption energies of the O atom were computed by Biemolt et al.[14] by means of nonrelativistic local spin-density approximation on a Cu_{11}(8, 3) cluster, which was chosen as the model of the Cu(111) surface, and the result was 4.16 eV, which agreed poorly with experiment.

It is easy to determine from Table 1 that the adsorption energies of an O atom on the Cu(111) surface follow the order fcc > hcp > bridge > top site. The preferred site is the 3-fold fcc hollow site with an adsorption energy of 4.42 eV, closely followed by the 3-fold hcp hollow site with an adsorption energy of 4.30 eV. The adsorption energy of atomic oxygen clearly decreases at the bridge site relative to that at the 3-fold hollow site. The least stable site is the top site with an adsorption energy of 3.41 eV. In a word, the fcc hollow site is slightly preferred to the hcp hollow site but is remarkably preferred to both the bridge site and the top site for the adsorption of an O atom on the Cu(111) surface. This agrees well with the general features of atomic adsorption on metal surfaces.[39]

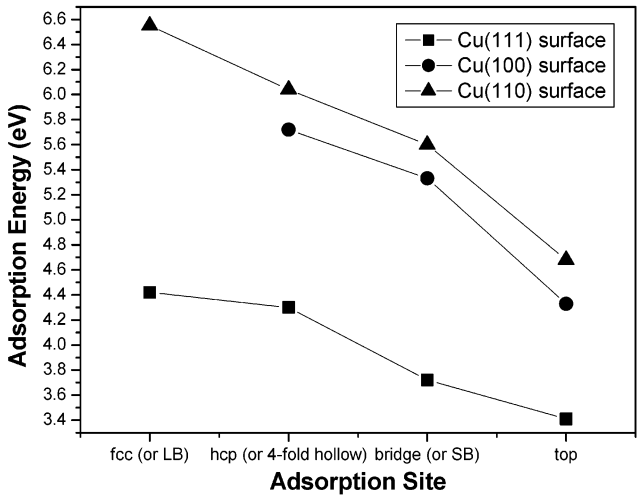

Figure 2. Adsorption energies of atomic oxygen on the Cu(111), Cu(100), and Cu(110) surfaces.

For the adsorption of an O atom on the Cu(100) surface, the data reported in Table 1 reveal that the 4-fold hollow site is the most stable site, with an adsorption energy of 5.72 eV (Z_{eq} = 0.93 Å). The studies conducted with normal photoelectron diffraction,[40] SEXAFS,[41] and, recently, STM[18] also show a preference for the 4-fold hollow site, with Z_{eq} values of ∼0.80, ∼0.70, and ∼0.70 Å, respectively. The theoretical studies from the many-electron embedding theory[15] and the ab initio molecular-orbital cluster-model approach[17] also indicate that the 4-fold hollow site is the preferred site, with adsorption energies of 6.10 eV ($Z_{eq} \approx$ 0.70 Å) and ∼5.56 eV ($Z_{eq} \approx$ 0.90 Å), respectively.

In the case of the Cu(110) surface, the O atom strongly prefers the long-bridge (LB) site. This agrees with various experimental evidence.[13,20] Frechard and van Santen[22] performed periodic DFT calculations for the adsorption of the oxygen atom on different sites of the unreconstructed Cu(110) surface and found that the most stable position for oxygen was the LB site (Z_{eq} = 0.54 Å).

In addition, the adsorption energies of atomic oxygen are comparatively shown in Figure 2. Close scrutiny of the data given in Table 1 and shown in Figure 2 permits us to draw the conclusion that the adsorption energy of the O atom is larger on the Cu(110) surface than on Cu(100) and Cu(111), giving the following order for the O−Cu(*hkl*) binding strengths: Cu(110) > Cu(100) > Cu (111).

3.2. Electron Configuration and Binding Characteristics of Atomic Oxygen with the Cu(*hkl*) Surfaces. In this section, we will take a closer look at the electron configuration and the binding characteristics of atomic oxygen on the Cu(*hkl*) surfaces. At the B3LYP/LANL2DZ-6-31G level, the NBO analysis has been carried out under the optimized geometries of the O−Cu(*hkl*) complexes. Only the representative results of the natural electron configuration are given for the O/Cu(111) system in Table 2 because of the similarity between the Cu(111), Cu(100), and Cu(110) surfaces. To address the binding characteristics, we report the results from NBO analysis for the Cu−O bond with the largest coefficient in Table 3.

First, we want to establish the dominant bonding mode (i.e., covalent or ionic) for O atoms on the Cu(*hkl*) surfaces. The natural charges listed in Table 1 suggest that the O atom forms essentially an ionic bond for all sites. Likewise, it can be found in our previous study[24] that atomic H forms essentially a covalent bond with the Cu(111) surface, whereas the S, O, and C atoms carry a relatively high negative charge and hence form

TABLE 2: Natural Electron Configuration of the O/Cu(111) System and the Cu(111) Cluster Model from First-Principles Density Functional Calculations[a]

adsorption site	atom	no.	natural electron configuration				
	Cu	1	[core]	4s(0.84)	3d(9.78)	4p(0.10)	5p(0.27)
top site	Cu	6	[core]	4s(0.81)	3d(9.95)	4p(0.03)	5p(0.03)
	Cu	8	[core]	4s(1.00)	3d(9.92)	4p(0.01)	5p(0.07)
	O	11	[core]	2s(1.97)	2p(5.11)		
	Cu	2	[core]	4s(0.58)	3d(9.86)	4p(0.03)	5p(0.05)
bridge site	Cu	6	[core]	4s(0.93)	3d(9.94)	4p(0.02)	5p(0.03)
	Cu	8	[core]	4s(0.95)	3d(9.93)	4p(0.01)	5p(0.08)
	O	11	[core]	2s(1.96)	2p(5.24)		
	Cu	2	[core]	4s(0.61)	3d(9.86)	4p(0.03)	5p(0.04)
Hcp hollow	Cu	6	[core]	4s(0.92)	3d(9.94)	4p(0.02)	5p(0.03)
site	Cu	8	[core]	4s(0.94)	3d(9.94)	4p(0.01)	5p(0.08)
	O	11	[core]	2s(1.95)	2p(5.26)		
	Cu	2	[core]	4s(0.58)	3d(9.88)	4p(0.03)	5p(0.04)
Fcc hollow	Cu	6	[core]	4s(0.89)	3d(9.95)	4p(0.02)	5p(0.03)
site	Cu	8	[core]	4s(0.94)	3d(9.93)	4p(0.01)	5p(0.08)
	O	11	[core]	2s(1.95)	2p(5.31)		
	Cu	1	[core]	4s(0.91)	3d(9.89)	4p(0.07)	5p(0.19)
Cu(111)	Cu	2	[core]	4s(0.75)	3d(9.94)	4p(0.01)	5p(0.05)
cluster	Cu	6	[core]	4s(1.08)	3d(9.93)	4p(0.01)	5p(0.04)
	Cu	8	[core]	4s(0.96)	3d(9.93)	4p(0.01)	5p(0.07)

[a] Number of atoms is the same as the label shown in Figure 1, and the tabulated number for O is 11 (not shown in Figure 1).

TABLE 3: NBO Analysis Results for the Cu−O Bond with the Largest Coefficient Computed for the O/Cu(111) System at the B3LYP/LANL2DZ-6-31G Level[a]

Cu(111) surface	Cu (%)				O (%)		
	occupancy	4s	4p	3d	occupancy	2s	2p
top	21.75	86.22	6.56	7.22	78.25	5.33	94.67
bridge	12.80	87.62	7.81	4.57	87.20	6.16	93.84
hcp hollow	10.84	89.63	8.09	2.28	89.16	4.70	95.30
fcc hollow	11.18	88.15	8.03	3.82	88.82	6.81	93.19

[a] Values given are for the optimized geometries of the Cu(111)−O complexes.

an ionic bond. Also, Arvanitis et al.[16] reported that the O−Cu(100) bond is essentially ionic. The binding of oxygen to the Cu(110) surface is completely ionic with hardly any trace of covalency, as demonstrated by Liem et al.[23] Considering the relationship between the amount of negative charge and the strength of the ionic bond, it may be rational to conclude that the strengths of ionic bonds for O atoms on the Cu(*hkl*) surfaces follow the order Cu(110) > Cu(100) > Cu(111).

It is well known that the electron configurations for the neutral oxygen atom and the copper atom in the ground state are [core]-2s(2.00)2p(4.00) and [core]4s(1.00)3d(10.00), respectively. The extended orbitals of Cu atoms are similar among the four kinds of adsorption sites but with somewhat of a difference in the electron distributions. Namely, the electrons in the 4s orbital of Cu(8) are all larger than those of the Cu(6) atoms corresponding to all of the sites, whereas for the 4p and 5p orbitals, the relationship is reversed. In addition, the sequence of Cu−O binding strengths, namely, fcc > hcp > bridge > top site, can also be found from the natural electron configuration of the O atom rather than Cu atoms because of the different coordination numbers of O atoms among the different sites. For instance, the electron number of the O atom in the fcc hollow site exceeds that in the top site by 0.18e (see Table 2). Close scrutiny of the data given in Table 2 permits us to draw the conclusion that the number of electrons in O 2p sharply changes after the O atom is adsorbed onto the Cu(111) surface, which is closely matched by the change in Cu(4s), which directly binds with an O atom (i.e., Cu(1) or Cu(2) shown in Table 2).

For an O atom on the fcc hollow site of the Cu(111) surface, the occupancy of the Cu atom in the Cu−O bond is 11.18% with contributions of Cu 4s (88.15%), Cu (4p) (8.03%), and Cu 3d (3.82%) and contributions to the Cu−O bond from O 2s and O(2p) of 6.81 and 93.19%, respectively, suggesting that the formation of the Cu−O bond is primary from the contributions of the Cu 4s and O 2p orbitals. Similar findings hold true for other sites on the Cu(111) surface. This is probably due to the interactions of the semifilled Cu 4s orbitals with O unfilled 2p orbitals. Also, our previous studies of N/M(111) (M = Cu, Ag, Au) systems[34] indicate that large contributions between the M *n*s and N 2p orbitals (n = 4, 5, and 6 for Cu, Ag, and Au, respectively) are the main characteristics of the M−N bond. In the case of an O atom on Cu(100), Ricart et al.[17] report that direct 3d involvement in the chemisorption bond is smaller than for the 4s orbital of the copper atom with the O 2p. For the adsorption of atomic oxygen on different sites of the Cu(110) surface, Frechard and van Santen[22] found that the formation of the Cu−O bond is essentially composed of the O 2p orbitals and the Cu 4s orbitals.

3.3. Surface Structure Sensitivity of the WGS Reaction over Cu(*hkl*) Surfaces. Manifesting a high level of accuracy in calculations of atomic and molecular chemisorption energies on metal surfaces, the UBI-QEP method demonstrated in every case[25,26] that it is a useful way to evaluate the activation barriers. On the basis of the reliable adsorption energies for the O atom from first-principle DFT calculations (Table 1), the adsorption energies of OH and H_2O are calculated using the UBI-QEP method. The calculated adsorption energies of OH and H_2O together with the experimental values of E_{ads}(H) can be used to determine the dissociation energy of adsorbed water ($D_{e,s}$). The scheme is

$$\begin{array}{ccccc} H_2O_s & \xrightarrow{D_{e,s}} & OH_s & + & H_s \\ \uparrow -E_{H_2O} & & \uparrow -E_{OH} & & \uparrow -E_H \\ H_2O_g & \xrightarrow[D_{e,g}]{} & OH_g & + & H_g \end{array} \qquad (2)$$

$$D_{e,s} = D_{e,g} + E_{H_2O} - E_{OH} - E_H \qquad (3)$$

where the term $D_{e,g}$ represents the dissociation energy of H_2O in the gas phase (i.e., 5.18 eV[28]) and E_{H_2O}, E_{OH}, and E_H are the adsorption energies of H_2O, OH, and H, respectively.

The analytical UBI-QEP equation relates the activation energy E^* to the adsorption energies of an adsorbate and its dissociation fragments on the surface. For the $H_2O_s \rightarrow OH_s + H_s$ reaction, the equation is given as

$$E^* = {}^1/_2\{D_{e,g} + [E_{OH}E_H/(E_{OH} + E_H)] + E_{H_2O} - E_{OH} - E_H\}$$
$$= {}^1/_2\{D_{e,s} + [E_{OH}E_H/(E_{OH} + E_H)]\} \qquad (4)$$

Here, the energy terms are shown by the scheme in eq 2.

We report the calculated adsorption energies, dissociation energies, and activation barriers in Table 4, together with available experimental data.

Because the interactions of H_2O with metal surfaces underline many important catalytic processes, they have been the subject of great interest and intense investigation.[42−44] Much experimental as well as theoretical work has been devoted to the study of the dissociation of H_2O on metal surfaces. Copper seems to

TABLE 4: Calculated Adsorption Energies (E_{ads}), Dissociation Energies ($D_{e,s}$), and Activation Barriers (E^*) for the Dissociation of H_2O[a]

	E_{ads} (O)	E_{ads} (OH)	E_{ads} (H)	E_{ads} (H_2O)	$D_{e,s}$	E^* (calcd)	E^* (exptl)	ref
Cu(111) surface	4.42	2.21	2.43	0.66	1.20	1.18	1.17	8
Cu(100) surface	5.72	3.22	2.55	1.23	0.64	1.03		
Cu(110) surface	6.55	3.90	2.62	1.68	0.34	0.95	0.90	9

[a] On the basis of the adsorption energy of atomic oxygen from Table 1, E_{ads}(OH) and E_{ads}(H_2O) are calculated using the UBI-QEP method (ref 26). The adsorption energies for the H atom are taken from ref 39. All units are eV.

be an interesting transition metal for the study of water adsorption because the interaction of H_2O with copper is directly relevant to the WGS reaction. To the best of our knowledge, there is no systematic study dealing with H_2O/Cu(*hkl*) systems. For a better understanding of the basic problems on copper surface, an investigation of water dissociation might be useful.

It is easy to find from Table 4 that the adsorption energies of H_2O on the Cu(*hkl*) surfaces follow the order Cu(110) > Cu(100) > Cu(111). The dissociation of H_2O to OH and H is highly endothermic in the gas phase ($D_{e,g} = 5.18$ eV). On the Cu(*hkl*) surfaces, there is a significant reduction in the dissociation energies owing to the presence of strong Cu−OH and Cu−H bonds, and the calculated activation barriers (1.18−0.95 eV) for the dissociation of an adsorbed water molecule agree well with the experimental range (1.17−0.90 eV).[8,9] Additionally, the present activation barrier (E^*) of water dissociation on the Cu(111) surface (1.18 eV) is consistent with the theoretical value (1.10 eV) from UBI-QEP microkinetic model analysis.[11] A comparison of the $D_{e,s}$ values given in Table 4 indicates that the water dissociation is still rather endothermic on Cu(111) (1.20 eV), followed by that on the Cu(100) surface (0.64 eV), whereas the dissociation of water on Cu(110) has the lowest dissociation energy of 0.34 eV and is the most favorable among the copper single-crystal surfaces considered here. Namely, the $D_{e,s}$ values vary in the order Cu(110) < Cu(100) < Cu(111). The same is true for the activation barriers (E^*). Spitzer et al.[42] concluded that the interaction of water with Cu(110) was stronger than with the Cu(100) surface from the ultraviolet photoelectron spectroscopy (UPS) and work-function measurements. They also pointed out that on the Cu(100) surface only water physisorbs, whereas on Cu(110), the formation of OH groups was found. This conclusion was supported by HREELS results from Prabhakaran et al.[45] and ESDIAD, LEED, and TPD results from Polak.[46] A majority of studies on Cu(110) have concluded either that water does not dissociate under UHV conditions[47,48] or that dissociation can be linked to the presence of surface defects or oxygen impurities.[46] Observations of water dissociation on Cu(111)[49] might also be linked to oxygen impurities,[50] as only the molecular adsorption of water has been observed in other studies of water on this surface.[51]

There is general agreement that water dissociation is the rate-determining step either in the formate mechanism or in the surface redox mechanism for the WGS reaction.[1−8,11] On the basis of the above-analyzed trends for the water molecular-dissociation energies and activation barriers, it can easily be concluded that the catalytic activity for the WGS reaction follows the order Cu(110) > Cu(100) > Cu(111). This is probably due to the fact that the (110) plane is so open that surface Cu atoms are much more coordinately unsaturated and hence more aggressive in chemisorptive bonding. These differences in activity between the open Cu(110) and Cu(100) surfaces and between Cu(110) and the more closely packed Cu(111) plane are consistent with observations that the high-area-supported Cu catalysts show increasing activity as the Cu particle size decreases.[12]

4. Conclusions

In the present work, first-principle density functional calculations together with the UBI-QEP method have been performed to investigate the surface structure sensitivity of the WGS reaction on the Cu(*hkl*) surfaces. Optimized results show that the O atom prefers the fcc hollow, 4-fold hollow site, and long-bridge site on the Cu(111), Cu(100), and Cu(110) surfaces, respectively. The results from NBO analysis indicate that the O atom forms largely an ionic bond with the Cu(*hkl*) surfaces. Large contributions between the Cu 4s and O 2p orbitals are the main characteristics of the Cu−O bond.

On the basis of the results from DFT calculations, the activation barriers and dissociation energies ($H_2O_s \rightarrow OH_s + H_s$) have been evaluated using the analytic UBI-QEP equation. The dissociation energy is shown to be an important factor distinguishing the water-dissociation processes on different single-crystal surfaces. It has been observed that the dissociation energies ($D_{e,s}$) for water follow the order Cu(110) < Cu(100) < Cu(111). The trend in the calculated dissociation energies implies that the WGS reaction rate might follow the order Cu(110) > Cu(100) > Cu(111) because of the fact that the water dissociation is the rate-determining step in the WGS reaction. The surface structure sensitivity of the WGS reaction over Cu(*hkl*) surfaces is in accord with the experimentally observed tendency.

Acknowledgment. This work was supported by the National Natural Science Foundation of China (grants no. 20273034), the Foundation of State Key Laboratory of C1 Chemistry & Technology (Taiyuan University of Technology), and the State Key Laboratory of Coal Conversion of China.

References and Notes

(1) Newsome, D. S. *Catal. Rev.—Sci. Eng.* **1980**, *21*, 275.
(2) van Herwijnen, T.; de Jong, W. A. *J. Catal.* **1980**, *63*, 83.
(3) Grenoble, D. C.; Estadt, M. M.; Ollis, D. F. *J. Catal.* **1981**, *67*, 90.
(4) Salmi, T.; Hakkarainer, R. *Appl. Catal.* **1989**, *49*, 285.
(5) Klier, K.; Young, C. W.; Nunan, J. G. *Ind. Eng. Chem. Fundam.* **1986**, *25*, 36.
(6) Fiolitakis, E.; Hofman, H. *J. Catal.* **1983**, *80*, 328.
(7) Handden, R. A.; Vandervell, H. D.; Waugh, K. C.; Webb, G. Proceedings of the 9th International Congress on Catalysis; Ottawa, Canada, 1988; Chemical Institute of Canada: Ottawa, Canada; Vol. 4, p 1853.
(8) Campbell, C. T.; Daube, K. A. *J. Catal.* **1980**, *104*, 109.
(9) Nakumura, J.; Campbell, J. M.; Campbell, C. T. *J. Chem. Soc., Faraday Trans.* **1990**, *86*, 2725.
(10) Chinchen, G. C.; Spencer, M. S.; Waugh, K. C.; Whan, D. A. *J. Chem. Soc., Faraday Trans. 1* **1987**, *83*, 2193.
(11) Fishtik I.; Datta R. *Surf. Sci.* **2002**, *512*, 229.
(12) Kuijpers, E. G. M.; Tjepkema, R. B.; van der Wal, W. J. J.; Mesters, C. M. A. M.; Spronck, S. F. G. M.; Geus, J. W. *Appl. Catal.* **1986**, *25*, 139.
(13) Besenbacher, F.; Nørskov, J. K. *Prog. Surf. Sci.* **1993**, *44*, 5.
(14) Biemolt, W.; Jansen, A. P. J.; Neurock, M.; van de Kerholf, G. J. C. S.; van Santen, R. A. *Surf. Sci.* **1993**, *287/288*, 183.
(15) Madhavan, P. V.; Newton, M. D. *J. Chem. Phys.* **1987**, *86*, 4030.
(16) Arvanitis, D.; Comelli, G.; Lederer, T.; Rabus, H.; Baberschke, K. *Chem. Phys. Lett.* **1993**, *211*, 53.
(17) Ricart, J. M.; Torras, J.; Illas, F.; Rubio, J. *Surf. Sci.* **1994**, *307−309*, 107.
(18) Kittel, M.; Polcik, M.; Terborg, R.; Hoeft, J.-T. et al. *Surf. Sci.* **2001**, *470*, 311.
(19) Döbler, U.; Baberschke, K.; Vvedensky, D. D.; Pendry, J. B. *Surf. Sci.* **1986**, *178*, 679.
(20) Robinson, A. W.; Somers, J. S.; Ricken, D. E.; Bradshaw, A. M.; Kilcoyne, A. L. D.; Woodruff, D. P. *Surf. Sci.* **1990**, *227*, 237.
(21) Ricart, J. M.; Torras, J.; Clotet, A.; Sueiras, J. E. *Surf. Sci.* **1994**, *301*, 89.
(22) Frechard, F.; van Santen, R. A. *Surf. Sci.* **1998**, *407*, 200.

(23) Liem, S. Y.; Kresse, G.; Clarke, J. H. R. *Surf. Sci.* **1998**, *415*, 194.
(24) Wang, G. C.; Jiang, L.; Cai, Z. S. et al. *J. Mol. Struct.*: *THEOCHEM* **2002**, *589*−*590*, 371.
(25) Shustorovich, E.; Baetzold, R. C. *Science (Washington, D.C.)* **1985**, *227*, 876.
(26) Shustorovich, E.; Sellers, H. *Surf. Sci. Rep.* **1998**, *31*, 1.
(27) van Santen, R. A.; Neurock, M. *Catal. Rev.*—*Sci. Eng.* **1995**, *37*, 557.
(28) *CRC Handbook of Chemistry and Physics*, 79th ed.; Lide, D. R., Ed.; CRC Press: Boca Raton, FL, 1998.
(29) *Phase Transitions and Adsorbate Reconstructuring at Metal Surfaces*; King, D. A., Woodruff, D. P., Eds.; Chemical Physics of Solid Surfaces; Elsevier: Amsterdam, 1994; Vol. 7.
(30) Becke, A. D. *J. Chem. Phys.* **1993**, *98*, 5648.
(31) Lee, C.; Yang, W.; Parr, R. G. *Phys. Rev. B* **1988**, *37*, 785.
(32) Frisch, M. J.; Trucks, G. W.; Schlegel, H. B.; Gill, P. M. W.; Johnson, B. G.; Robb, M. A.; Cheeseman, J. R.; Keith, T.; Petersson, G. A.; Montgomery, J. A.; Raghavachari, K.; Al-Laham, M. A.; Zakrzewski, V. G.; Ortiz, J. V.; Foresman, J. B.; Cioslowski, J.; Stefanov, B. B.; Nanayakkara, A.; Challacombe, M.; Peng, C. Y.; Ayala, P. Y.; Chen, W.; Wong, M. W.; Andres, J. L.; Replogle, E. S.; Gomperts, R.; Martin, R. L.; Fox, D. J.; Binkley, J. S.; Defrees, D. J.; Baker, J.; Stewart, J. P.; Head-Gordon, M.; Gonzalez, C.; Pople, J. A. *Gaussian 94*, revision E.3; Gaussian, Inc.: Pittsburgh, PA, 1995.
(33) Hay, P. J.; Wadt, W. R. *J. Chem. Phys.* **1985**, *82*, 299.
(34) Wang, G. C.; Jiang, L.; Cai, Z. S. et al. Submitted for publication.
(35) Foster, J. P.; Weinhold, F. *J. Am. Chem. Soc.* **1980**, *102*, 7211.
(36) Reed, A. E.; Weinhold, F. *J. Chem. Phys.* **1983**, *78*, 4066.
(37) Reed, A. E.; Weistock, R. B.; Weinhold, F. *J. Chem. Phys.* **1985**, *83*, 735.
(38) Glendening, E. D.; Reed, A. E.; Carpenter, J. E.; Weinhold, F. *NBO*, version 3.1.
(39) *The Nature of the Surface Chemical Bond;* Rhodin, T. N., Ertl, G., Eds.; North-Holland Publishing Company: Amsterdam, 1979.
(40) Tobin, J. G.; Klebanoff, L. E.; Rosenblatt, D. M. et al. *Phys. Rev. B* **1982**, 26, 7076.
(41) Dobler, U.; Baberschke, K.; Stohr, J.; Outka, D. A. *Phys. Rev. B* **1985**, *31*, 2532.
(42) Spitzer, A.; Ritz, A.; Lüth, H. *Surf. Sci.* **1985**, *152*/*153*, 543.
(43) Thiel, P. A.; Madey, T. E. *Surf. Sci. Rep.* **1987**, *7*, 211.
(44) Henderson, M. A. *Surf. Sci. Rep.* **1998**, *46*, 1.
(45) Prabhakaran, P.; Sen, P.; Rao, C. N. R. *Surf. Sci.* **1986**, *169*, L301.
(46) Polak, M. *Surf. Sci.* **1994**, *321*, 249.
(47) Kubota, J.; Kondo, J.; Domen, K.; Hirose, C. *Surf. Sci.* **1993**, *295*, 169.
(48) Lackey, D.; Schott, J.; Sass, J. K.; Woo, S. I.; Wagner, F. T. *Chem. Phys. Lett.* **1991**, *184*, 277.
(49) Au, C.-T.; Breza, J. K.; Roberts, M. W. *Chem. Phys. Lett.* **1979**, *66*, 340.
(50) Stickney, J. L.; Ehlers, C. B.; Gregory, B. W. *ACS Symp. Ser.* **1988**, *378*, 99.
(51) Bange, K.; Doehl, R.; Grider, D. E.; Sass, J. K. *Vacuum* **1983**, *33*, 757.
(52) Giamello, E.; Fubini, B.; Lauro, P.; Bossi, A. *J. Catal.* **1984**, *87*, 443.